

Coordinated Operation of Multi-Integrated Energy System Based on Linear Weighted Sum and Grasshopper Optimization Algorithm

JINGLU LIU¹, ANNA WANG, YANHUA QU¹, AND WENHUI WANG

College of Information Science and Engineering, Northeastern University, Shenyang 110819, China

Corresponding author: Jinglu Liu (bradybest@163.com)

ABSTRACT Aiming at tapping the potential of energy complementary, maximizing renewable energy sources utilization and jointly minimizing the operating cost, a coordinated operation model of a multi-integrated energy system based on linearized coupling relationship is established in this paper. In order to establish an accurate model for interconnected energy hubs, an integrated strategy is proposed by the combination of the linear weighted sum and grasshopper optimization algorithm to solve the energy management problem, which improves comprehensive energy efficiency and realize regional coordination optimization. Eventually, the case study indicates that the operating cost of the multi-integrated energy system with coordination is reduced by nearly 3.2%, which can effectively validate the scalability, flexibility, and economic performance of the presented integrated strategy.

INDEX TERMS Multi-integrated energy system, linearized coupling relationship, energy hub, grasshopper optimization algorithm.

I. INTRODUCTION

With rapid escalation in energy consumption, as well as sharp increase in the burden on the large-scale integration of renewable energy sources (RES). The integrated energy system (IES), as an effective way of integrating and utilizing multiple types of flexible energy sources such as electricity, natural gas, heat and so on, is able to improve the overall energy utilization efficiency and mitigate the operational challenges of multiple energy supply [1].

At local level, for an IES covering a small area, the energy conversion components can be modeled using the concept of energy hub (EH) [2]. Since the scale of the local community, commercial and industrial complexes are usually at the district level. If these complexes are controlled by a single isolated IES, the computational complexity increases significantly as the scale of the IES expands. The conventional independent operation of IES can no longer satisfy the requirements of multi-energy complementary. It is appropriate to construct regional multi-integrated energy system (multi-IES) on the distribution network.

In recent years, several studies have been conducted to optimize the operation and planning of IES. A unified steady-state power flow analysis considering electrical, natural gas and district heating networks is proposed in [3].

Shao *et al.* applied an mixed integer linear programming (MILP) method based EH for calculating the optimal power flow in IES are illustrated in [4] and a state variable-based linear energy hub model is also developed. Reference [5] proposes an interval optimization based coordinated operating strategy for a gas-electricity IES. Reference [6] provides a comprehensive operational flexibility evaluation of different IES options. A hierarchical multi-agent system control structure were used for IES optimal operation in [7]. In [8], a combined heat and power dispatch is formulated to coordinate the operation of electric power system and district heating system. Reference [9] proposes a unified operation and planning optimization methodology for distributed IES with the aim of assessing flexibility embedded in both operation and investment stages subject to long-term uncertainties. Reference [10] optimizes the conflicting benefits of the electricity network and gas network for daily operation of the IES using a coordinated scheduling strategy. Reference [11] further considers the dynamic optimal gas flow on pipeline networks and the optimal power flow in power network which forms a unified scheduling method. The optimal operation of gas-fired power plants in electricity market is described by IESs in [12]. Reference [5] introduces an interval optimization based coordinated operating strategy

for the gas-electricity IES to describe the probability distribution of wind power output. Reference [13] establishes a multi-objective optimization model for the combined gas and electricity network planning and the stochastic characteristics of wind power, and the optimization problem is solved by the Elitist Non-dominated Sorting Genetic Algorithm II. Reference [14] further adds the water network constraints to the IES, and optimizes the optimal network capacity and distribution of the CHP-based DG based on urban energy distribution networks. A hierarchical approach for a community IES is designed in [15], considering demand response and the distribution of power and gas flow. Reference [16] further considers the influence of power distribution network reconfiguration on IES with cogeneration. In [17], a decentralized algorithm is proposed for the integrated power and heat scheduling based on Benders decomposition. Shabanpour-Haghighi and Seifi [3] presented an integrated framework based on the Newton-Raphson technique to solve the operation of IES including electrical, natural gas, and heat carriers.

In addition to the research that has focused on the optimal operation and planning of IES, the optimization modeling of IES have been reported in several studies. In [18], a combined gas and electricity network expansion planning model is developed. Gas-fired generation plants are considered as linkages between the two networks. A security-constrained bi-level economic dispatch model for IES is proposed in [19]. A combined gas and electricity networks expansion model is proposed in [20]. The results show that demand-side response plays a crucial role in the improvement of security of gas supply. Reference [21] constructs a day-ahead coordinated stochastic model considering random outages of generating units and transmission lines, and random errors in forecasting the day-ahead hourly loads. In [22], a multi-objective model is introduced to describe the optimization problem of IES, and the dynamic security of electricity network is evaluated. In [23], a stochastic model is established to analyze the stabilization effect of gas-electricity coordinated scheduling on wind power fluctuation. Reference [24] proposes a probabilistic available transfer capability model considering the static security constraints and uncertainties of electricity-gas IESs. Reference [25] proposes a planning expansion planning model for the IES which can have lower investment costs. Reference [26] presents a multi-temporal simulation model to analyze the IES, in which the related equations are solved by Newton Raphson method. Interactions in a district electricity and heating systems is analyzed in [27] considering the time-scale characteristics. Li *et al.* [28] proposed a low-carbon stochastic optimal operation model for IES with the comprehensive consideration of renewable generation, carbon-capture-based power-to-gas technology, and the combined power and heat units. Qiu *et al.* [29] provided a linear expansion model of IES to minimize the overall capital and operational costs for the coupled gas and power systems. Zhang *et al.* [30] studied the optimal expansion planning of EH with multiple energy systems. A smart EH

is presented in [31], modify the conventional DR programs in smart grid, and a distributed algorithm is developed to determine the equilibrium. Beyond planning for a single EH, Pazouki *et al.* [32] proposed optimal CHP placement and sizing in a multiple energy network considering the operation costs, power loss, network reliability, and voltage penalty. Reference [30] expanded the concept of EH by determining appropriate investment candidates for generating units, transmission lines, natural gas furnaces, and CHPs. Orehounig *et al.* [33] deployed the energy hub concept at the urban level, considering the integration of renewable sources at residential and commercial buildings and neighborhood scale.

It is worth noting that all aforementioned research are focused on the traditional independent optimal operation of IES and the optimal operation of multi-IES and inter-connection between EHs has not been accurately investigated or modeled. To address the issue of the multi-energy complementary among EHs while realizing regional coordination optimization and improving comprehensive energy efficiency. The major contributions of this paper are summarized as follows:

On the one hand, a linearized method of modeling EH is proposed to analyze the dynamic characteristics of energy conversion devices. Energy conversions are regarded as coupling components to transfer the RES fluctuation to the cooling or heating system.

On the other hand, the industrial EH (I-EH) model commercial EH (C-EH) model and residential EH (R-EH) model are added into coordinated operation optimization of modeling multi-IES respectively. In addition, an integrated strategy is proposed by combination of linear weighted sum (LWS) and grasshopper optimization algorithm (GOA) for multi-IES operation problem analysis. The comparison of results with other techniques already available in the literature like mixed integer linear programming (MILP) shows that LWSGOA algorithm has better strength and more potential than MILP.

The remainder of this paper is outlined as follows:

In Section II, the mathematical EH models based on linearized coupling relationship are developed, respectively. Section III provides the modeling framework for the coordinated operation of multi-IES. In addition, the objective function, the associated constraints and LWSGOA algorithm are described in this section. In section IV, the case study is simulated on multi-IES consisting of three interconnected EHs. The conclusion of this paper is summarized in Section V

II. LINEARIZED COUPLING MODEL OF EH

The concept of EH is used to describe the energy coupling relationship in the IES. The EH is made up of micro-grid, micro-gas system and micro-heat system and integrates various forms of energy such as electricity, natural gas, hydrogen, renewable energy sources like wind power and photovoltaic generation. The regional IES can effectively adjust the uncertainty caused by the RES integration into the power system, and help solve the problem of power system stability.

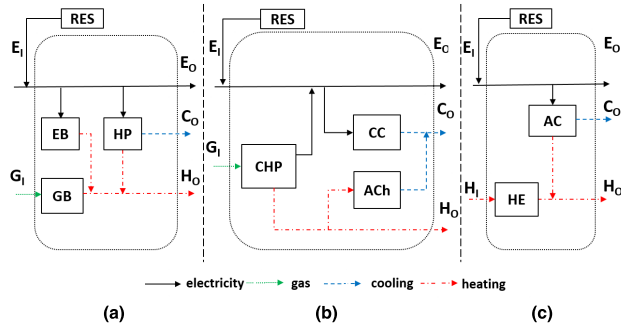


FIGURE 1. The structures of I-EH, C-EH and R-EH. (a) I-EH. (b) C-EH. (c) R-EH.

For proper energy conversion and distribution, the structure of I-EH, C-EH and R-EH are established respectively, as illustrated in Fig. 1. The figure shows the connection between the various devices in the IES and the energy flow.

Considering the diversification of energy are connected through conversion devices, the converter of multiple energy flow is abstracted as an energy conversion efficiency matrix. The input E_1^t, G_1^t are supply of electricity and natural gas. The output E_0^t, H_0^t, C_0^t , which are energy demand of electricity, heat, and cold, can be met by the coordinating of the energy conversion devices.

A. LINEARIZED COUPLING MODEL OF EHS

Fig. 1 (a) consists of heat pump (HP), electrical boiler (EB), and gas boiler (GB). Heat energy is easy to recover in form of hot water compared with electricity, thus could provide huge space for the utilization of RES. E_0^t is supplied through the utility grid (UG) E_1^t and RES, H_0^t is provided by GB $H_{GB,O}^t$ and HP $H_{AC,O}^t$, the EB $H_{EB,O}^t$ is utilized to serve as auxiliary sources to meet heating load, C_0^t is supplied by HP $C_{HP,O}^t$.

$$\begin{bmatrix} E_0^t \\ H_0^t \\ C_0^t \\ H_{GB,O}^t \\ H_{EB,O}^t \\ H_{HP,O}^t \\ C_{HP,O}^t \end{bmatrix} = \begin{bmatrix} 0 & 1 & 0 & -1 & -1 \\ 0 & 0 & \eta_{GB,GH} & \eta_{EB,EH} & \eta_{HP,EH} \\ 0 & 0 & 0 & 0 & \eta_{HP,EC} \\ 0 & 0 & \eta_{GB,GH} & 0 & 0 \\ 0 & 0 & 0 & \eta_{EB,EH} & 0 \\ 0 & 0 & 0 & 0 & \eta_{HP,EH} \\ 0 & 0 & 0 & 0 & \eta_{HP,EC} \end{bmatrix} \begin{bmatrix} G_1^t \\ E_1^t \\ G_{GB,I}^t \\ E_{EB,I}^t \\ E_{HP,I}^t \end{bmatrix} \quad (1)$$

Where $\eta_{GB,GH}$ is the conversion efficiency of GB; $\eta_{EB,EH}$ refers to the EB efficiency from electricity input to heat output; $\eta_{HP,EH}, \eta_{HP,EC}$ are the heating and cooling efficiency of HP, respectively.

Fig. 1 (b) contains combined heat and power (CHP) unit, absorption chiller (ACh), and compression chiller (CC). $E_{CCHP,O}^t, H_{CCHP,O}^t$ are the proportion of natural gas consumption for electricity and heat, respectively; $C_{ACh,O}^t$ is the partition coefficient of ACh using the waste heat by CHP, which can be converted into cold energy to meet cooling demand. The cascade utilization of waste heat and surplus

electricity can be beneficial to improve the energy efficiency.

$$\begin{bmatrix} E_0^t \\ H_0^t \\ C_0^t \\ E_{CHP,O}^t \\ H_{CHP,O}^t \\ C_{CC,O}^t \\ C_{ACh,O}^t \end{bmatrix} = \begin{bmatrix} 0 & 1 & \eta_{CHP,GE} & -1 & 0 \\ 0 & 0 & \eta_{CHP,GH} & 0 & -1 \\ 0 & 0 & 0 & \eta_{CC,EC} & \eta_{ACh,HC} \\ 0 & 0 & \eta_{CHP,GE} & 0 & 0 \\ 0 & 0 & \eta_{CHP,GH} & 0 & 0 \\ 0 & 0 & 0 & \eta_{CC,EC} & 0 \\ 0 & 0 & 0 & 0 & \eta_{ACh,HC} \end{bmatrix} \begin{bmatrix} G_1^t \\ E_1^t \\ G_{CHP,I}^t \\ E_{CC,I}^t \\ H_{ACh,I}^t \end{bmatrix} \quad (2)$$

Where $\eta_{CHP,GE}, \eta_{CHP,GH}$ are the electrical and thermal efficiency of CHP, respectively; $\eta_{ACh,HC}$ is the cooling efficiency of ACh; $\eta_{CC,EC}$ refers to the energy conversion efficiency of CC from electricity to cooling.

Fig. 1 (c) consists of air conditioner (AC) and heat exchanger (HE). EH converts heat by HE and combines AC to meet heating and cooling demands.

$$\begin{bmatrix} E_0^t \\ H_0^t \\ C_0^t \\ H_{HE,O}^t \\ H_{AC,O}^t \\ C_{AC,O}^t \end{bmatrix} = \begin{bmatrix} 0 & 1 & -1 & 0 \\ 0 & 0 & \eta_{AC,EH} & \eta_{HE,HH} \\ 0 & 0 & \eta_{AC,EC} & 0 \\ 0 & 0 & 0 & \eta_{HE,HH} \\ 0 & 0 & \eta_{AC,EH} & 0 \\ 0 & 0 & \eta_{AC,EC} & 0 \end{bmatrix} \begin{bmatrix} G_1^t \\ E_1^t \\ E_{AC,I}^t \\ H_{HE,I}^t \end{bmatrix} \quad (3)$$

Where $\eta_{AC,EH}, \eta_{AC,EC}$ are the energy conversion efficiency (electricity-heating and electricity-cooling) of AC, respectively.

B. PHOTOVOLTAIC PANELS AND WIND TURBINE

When considering the uncertainty of RES, the output power of RES were modeled as stochastic parameters. The power output of PV depends on the amount of solar irradiance, temperature changes and efficiency changes. The output of PV can be expressed as follows:

$$I_0(t) = \frac{I_{SC}(t)}{e^{\frac{qV_{oc}(t)}{nkT}} - 1} \times \frac{T^{\frac{3}{n}}}{t} \times e^{\frac{qV_g(t)}{nk(\frac{1}{T} - \frac{1}{T_0})}} \quad (4)$$

$$I_L(t) = I_{SC}(t) \times S + K_0(T - t) \quad (5)$$

$$I(t) = I_L(t) - I_0(t) \left(e^{\frac{q(V+IR_s)}{nkT}} - 1 \right) \quad (6)$$

$$P_{PV} = \max\{I(t) \times V_g\} \times 90\% \quad (7)$$

Where K_0 is the current/temperature coefficient, S is the solar irradiance, k is the Boltzmann constant, q is the electron, n is the quality factor of the diode, $I_L(t)$ is the photocurrent deciding by the temperature t , $I_0(t)$ is the saturation

current of diode deciding by the temperature t , V_g is the open circuit voltage, $I_{SC}(t)$ is the working current deciding by the temperature t , $V_{oc}(t)$ is the working voltage deciding by the temperature t , R_s is the resistance of the source.

The wind speed and technical specifications can cause power output variations of wind turbine (WT). The output can be expressed as follows:

$$P_{WT} = \begin{cases} 0 & V < V_{Cin} \text{ or } V < V_{Cout} \\ 0.5 \times A_{WT} \times C_{WT} \times \rho_{WT} \times v_{WT}^3 & V_{Cin} < V < V_{rated} \\ P_{rated} & V_{rated} < V < V_{Cout} \end{cases} \quad (8)$$

Where A_{WT} is the swept area, C_{WT} is the wind energy utilization coefficient, ρ_{WT} is the air density and v_{WT} is the wind speed. V is the wind speed, V_{Cin} is the cut-in speed, V_{rated} is the rated speed, V_{Cout} is the cut-out speed, and P_{rated} is the rated output power.

III. MODELING OF COORDINATED OPERATION

In this study, an optimal model of three interconnected EHs representing multi-IES is established as Fig. 2. Each EH can exchange energy with each other to fulfill the load-generation constraints. In proposed model, the multi-IES will improve the comprehensive energy efficiency and bring better economical circumstance for those of EHs in which the value of generation is higher than load consumption.

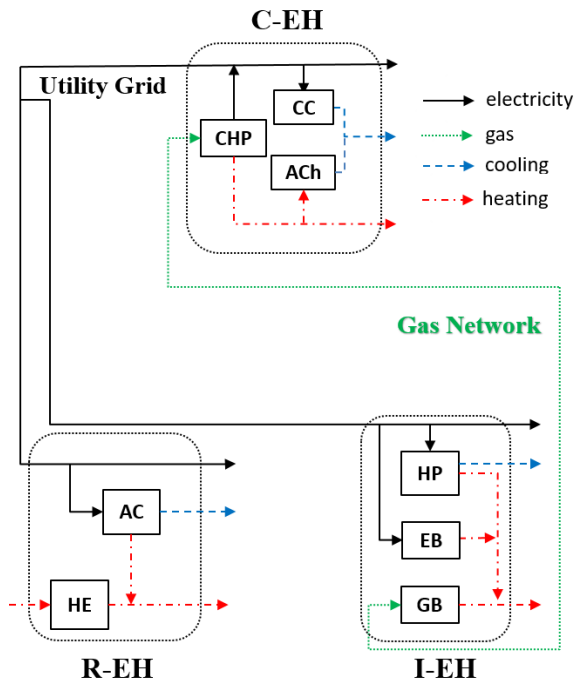


FIGURE 2. Planning model of the multi-IES.

The Fig. 2 depicts how the proposed planning model works. The multi-IES topology consists three EHs combined gas network and utility grid. The EH is tied to adjacent EHs through energy networks, which can form the coupling and

connectivity matrices of the multi-IES. Each EH performs its own optimal operation or perform energy exchanging in the form of energy trading with another EH. If extra energy for any carrier is more than the required amount in an EH, it will be transported to the other EHs in the network where there is deficit. The model can be extended to a very big network with numerous EHs.

A. OBJECTIVE FUNCTION

Co-operation multi-IES will affect the distribution of the load on each energy source. The objective function aims at minimizing the operating cost of multi-IES, which consists of electricity, natural gas and heat purchasing cost. The objective function of coordinated operation optimization model is as follows:

$$C_{Total} = \sum_{t=1}^{T=24} \left[C_{E,net} \sum E_{net,i}^t + C_{G,net} \sum G_{net,i}^t CV \right] - C_{H,net} H_{I-EX}^t - C_{E,net} E_{C-EX}^t \quad (9)$$

Where CV is calorific value; $C_{E,net}$ and $C_{G,net}$ are the electricity price and natural gas price respectively. Each EH can purchase heat from heat sources owned by other EHs at a fixed contract price $C_{H,net}$.

B. CONSTRAINT CONDITIONS

The constraints related to energy balance of different energy carriers, transmission line, gas pipeline and converter limitations of the inputs and outputs are included as equality and inequality constraints. The demand-supply balance equations of the I-EH can be expressed as follows:

$$E_{I-EX}^t + \sum E_{HP}^t + \sum E_{EB}^t = E_{net}^t + \sum E_{RES}^t \quad (10)$$

$$H_{I-EX}^t + H_{I-EX}^t = \eta_{HP,EH} \sum E_{HP}^t + \eta_{EB,EH} \times \sum E_{EB}^t + \eta_{GB,GH} \sum G_{GB}^t \quad (11)$$

$$C_{I-EX}^t = \eta_{HP,EC} \sum E_{HP}^t \quad (12)$$

Eq. (10) expresses the demand-supply balance for power of the I-EH. The input power is consisted of purchased power from $UG E_{net}^t$ and $RES E_{RES}^t$. The output power is consisted of electrical load, electricity for HP E_{HP}^t and EB E_{EB}^t as the auxiliary heat energy source. Eq. (11) states the heat generated by GB G_{GB}^t , EB E_{EB}^t and HP E_{HP}^t should satisfy heating load. Eq. (12) demonstrates the balance for cooling power between the HP and cooling demand. The energy balance equations of the C-EH can be formulated as follows:

$$E_{C-EX}^t + E_{C-EX}^t + \sum E_{CC}^t = E_{net}^t + \sum E_{RES}^t + \eta_{CHP,GE} \sum G_{CHP}^t \quad (13)$$

$$H_{C-EX}^t + \sum H_{ACh}^t = \eta_{CHP,GH} \sum G_{CHP}^t \quad (14)$$

$$C_{C-EX}^t = \eta_{CC,EC} \sum E_{CC}^t + \eta_{ACh,HC} \sum H_{ACh}^t \quad (15)$$

On one hand, the input energy is consisted of purchased power from UG E_{net}^t , RES E_{RES}^t , energy generated by CHP E_{CHP}^t , CC E_{CC}^t and ACh H_{ACh}^t . The CC could compensate for the insufficient cooling energy from ACh and moderates the electrical and thermal energy consumption and production. On the other hand, the output energy are the electricity, heating and cooling loads. The R-EH balance constraints can be expressed as follows:

$$E_{R-EH}^t + \sum E_{AC}^t = E_{net}^t + \sum E_{RES}^t + E_{C-EX}^t \quad (16)$$

$$H_{R-EH}^t = \eta_{AC,EH} \sum E_{AC}^t + \eta_{HE,HH} H_{I-EX}^t \quad (17)$$

$$C_{R-EH}^t = \eta_{AC,EC} \sum E_{AC}^t \quad (18)$$

Constraints (16-18) denote that the outputs of the R-EH should satisfy the electrical, heating and cooling loads.

$$0 \leq \left| \sum E_{net}^t \right| \leq E_{net}^{\max} \quad (19)$$

$$0 \leq \sum G_{net}^t \leq G_{net}^{\max} \quad (20)$$

The constraints (19-20) indicate the limitation that the energy from the networks cannot exceed the permitted capacities of the transmission line and gas pipeline, respectively.

$$0 \leq E_{HP}^t \leq E_{HP}^{\max} \quad (21)$$

$$0 \leq E_{EB}^t \leq E_{EB}^{\max} \quad (22)$$

$$0 \leq G_{GB}^t \leq G_{GB}^{\max} \quad (23)$$

$$G_{CHP}^{\min} \leq G_{CHP}^t \leq G_{CHP}^{\max} \quad (24)$$

$$\tau_{down} \leq \left| G_{CHP}^t - G_{CHP}^{t-1} \right| \leq \tau_{up} \quad (25)$$

$$0 \leq H_{ACh}^t \leq H_{ACh}^{\max} \quad (26)$$

$$0 \leq E_{CC}^t \leq E_{CC}^{\max} \quad (27)$$

$$0 \leq E_{AC}^t \leq E_{AC}^{\max} \quad (28)$$

Where E_{HP}^{\max} , E_{EB}^{\max} , G_{GB}^{\max} , G_{CHP}^{\max} , G_{CHP}^{\min} , H_{ACh}^{\max} , E_{CC}^{\max} and E_{AC}^{\max} are limited by the rated capacity of the devices; τ_{up} , τ_{down} are the ramp constraints of CHP unit. Formulas (10)-(28) constitute the coordinated operation optimization model of multi-IES with linear objective functions and constraints, in addition to the energy flow calculation (19) and (20) considered for traditional coordinated operation, the multi-energy coupling of the energy conversion is also included, such as Formulas (21)-(28).

C. LWSGOA ALGORITHM

The adaptive mechanism in GOA [34] has been proven to balance exploration and exploitation and cope with the difficulty of multi-objective search space while outperforming other optimization methods. The GOA requires all particles to get involved in updating the position of each particle, which can avoid trapping in local minima and premature convergence.

$$X_i^d = c \left(\sum_{\substack{j=1 \\ j \neq i}}^N c \frac{ub_d - lb_d}{2} s \left(x_j^d - x_i^d \right) \frac{x_j - x_i}{d_{ij}} \right) + \hat{T}_d \quad (29)$$

$$s(r) = fe^{\frac{-r}{\tau}} - e^{-r} \quad (30)$$

Where $d_{ij} = |x_j - x_i|$ denotes the distance between i th and j th grasshopper, ub_d and lb_d are the upper and lower bound in the d th dimension, respectively, c is a decreasing coefficient to shrink the comfort zone, repulsion zone, and attraction zone, The gravity is ignored and the wind direction is always towards the target \hat{T}_d , s defines the strength of social forces, f indicates the intensity of attraction, l is the attractive length scale. The inner c is referred to the adaptive parameter which can decrease repulsion or attraction force between grasshoppers and the outer c reduces the search coverage around the target as the iteration count increases. In order to enhance local search ability, improve accuracy and speed of convergence, the improved inertia weight is introduced to the GOA algorithm.

$$c = c \max - (c \max - c \min) \left(\frac{iter}{iter_{\max}} \right)^{\frac{1}{iter}} \quad (31)$$

Where $c \max$ is the maximum value, $c \min$ is the minimum value, $iter$ indicates the current iteration, $iter_{\max}$ is the maximum number of iterations.

To apply GOA to the IES of multi-IES, the LWSGOA is proposed as follows to solve optimization problem. The LWS algorithm changes the multiple objective problems into the optimization of a single objective model. The weights of objectives ω_i multiplies each objective function f_i to make the structure of the objective function as follows [35]:

$$\begin{cases} \min \sum_{i=1}^k \omega_i f_i(X) & i = 1, 2, \dots, p \\ \omega_i \geq 0, & \sum_{i=1}^k \omega_i = 1 \end{cases} \quad (32)$$

s.t. $\begin{cases} h_j(X) = 0 \\ g_k(X) \leq 0 \end{cases}$

$f(X)$ is the total cost of multi-IES, $g_k(X)$ ($k = 1, 2, \dots, m$) are inequality constraints, $h_j(X)$ ($j = 1, 2, \dots, n$) are equality constraints, and m, n are the numbers of inequality constraints and equality constraints respectively.

IV. CASE STUDY AND SIMULATION RESULTS

A. SIMULATION SETUP

An optimal model of three interconnected EHs representing multi-IES is established as the case study. Fig. 3 (a) (b) (c) show forecast consumption curves for electrical, heating and cooling daily loads of three EHs during typical days, respectively.

The common characteristics of the three EHs are that the EHs tend to buy cheap electricity from UG in the valley period and tend to use their own RES generations. The parameters of the components in the multi-IES, including capacities and efficiencies, are listed in Table 1.

The number and installed capacity of energy devices are given in Table 2-4.

The outputs of WTs and PVs of three EHs is shown in Fig. 4.

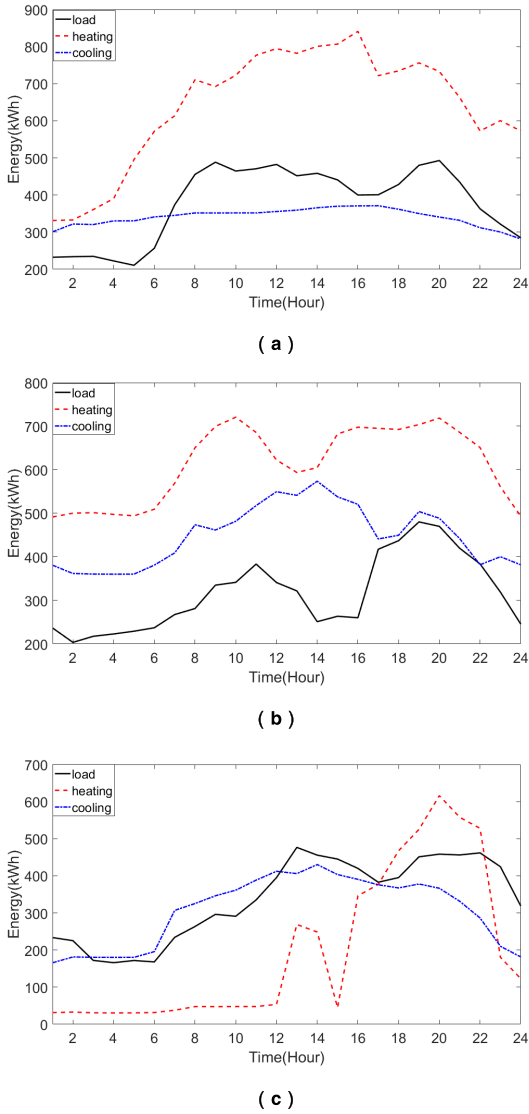


FIGURE 3. Daily energy demands for I-EH, C-EH and R-EH. (a) I-EH. (b) C-EH. (c) R-EH.

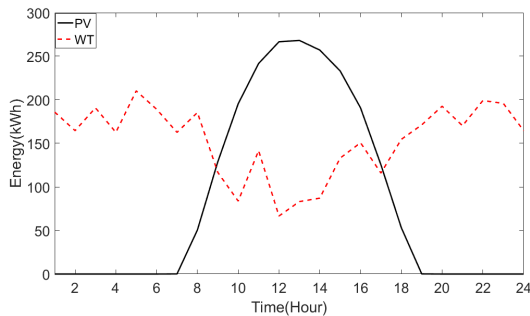


FIGURE 4. RES outputs for EHs.

The hourly energy price for multi-IES is comprised by the time-of-use electricity pricing schemes with fixed pricing scheme for the natural gas and heat, as shown in Fig. 5. Different electrical prices are set for different periods, reflecting the variations of electrical load.

TABLE 1. Parameters of energy conversion devices in multi-IES.

Component	Capacity (kW)	Efficiency
CHP	$E_{CHP,O}^{\max} = 60$	$\eta_{CHP,GE} = 0.3$
	$H_{CHP,O}^{\max} = 90$	$\eta_{CHP,GH} = 0.45$
AC	$H_{AC,O}^{\max} = 600$	$\eta_{AC,EH} = 3$
	$C_{AC,O}^{\max} = 700$	$\eta_{AC,EC} = 3.5$
HP	$H_{HP,O}^{\max} = 200$	$\eta_{HP,EH} = 2$
	$C_{HP,O}^{\max} = 250$	$\eta_{HP,EC} = 2.5$
CC	$C_{CC,O}^{\max} = 600$	$\eta_{CC,EC} = 3$
EB	$H_{EB,O}^{\max} = 270$	$\eta_{EB,EH} = 0.9$
GB	$H_{GB,O}^{\max} = 240$	$\eta_{GB,GH} = 0.8$
ACh	$C_{ACh,O}^{\max} = 210$	$\eta_{ACh,HC} = 0.7$
HE		$\eta_{HE,HH} = 0.95$

TABLE 2. Energy devices and parameters in I-EH.

Component	Total number	Installed capacity (kW)
Wind turbines	2	100
Photovoltaic panels	2	150
HP	1	200
EB	1	270
GB	2	240

TABLE 3. Energy devices and parameters in C-EH.

Component	Total number	Installed capacity (kW)
Wind turbines	2	100
Photovoltaic panels	2	150
CHP	6	90
CC	1	600
ACh	2	210

TABLE 4. Energy devices and parameters in R-EH.

Component	Total number	Installed capacity(kW)
Wind turbines	2	100
Photovoltaic panels	2	150
AC	1	700

B. ENERGY COMPLEMENTARITY OF THE MULTI-IES

In Multi-IES, whether involved in energy complementarity is considered and the dynamic characteristics of energy conversion devices are analyzed. The optimal output of the energy conversions are given, as shown in Fig. 6-14, demonstrating that there is a huge potential for energy complementarity in Multi-IES.

The electrical power of RES is used to supply the electrical load of I-EH and the remainder of available electrical energy can be converted to heat energy through EB and HP or

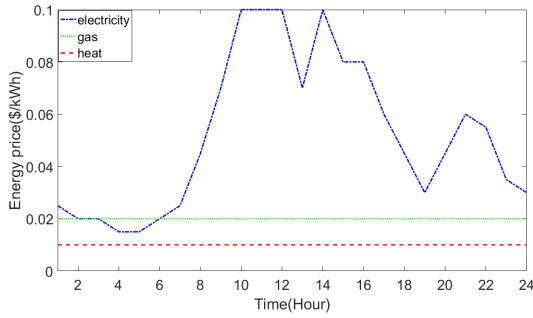


FIGURE 5. Hourly energy price of EHs.

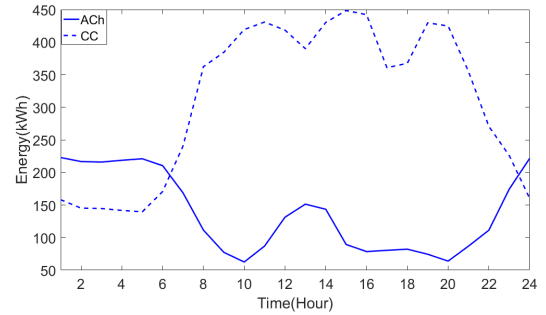


FIGURE 9. Cooling conversion in C-EH.

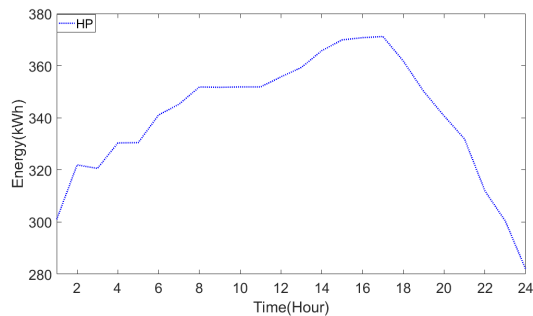


FIGURE 6. Cooling conversion in I-EH.

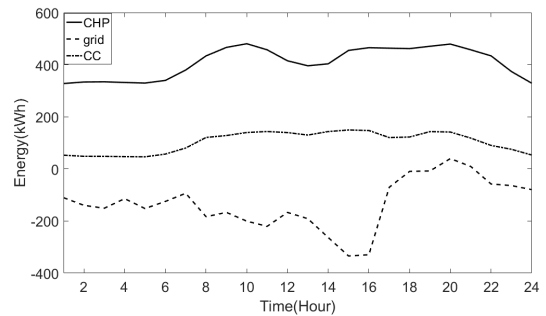


FIGURE 10. Electricity conversion in C-EH.

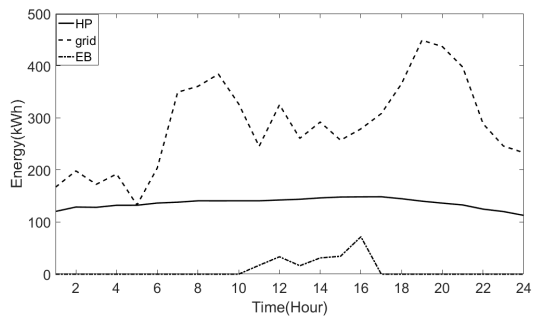


FIGURE 7. Electricity conversion in I-EH.

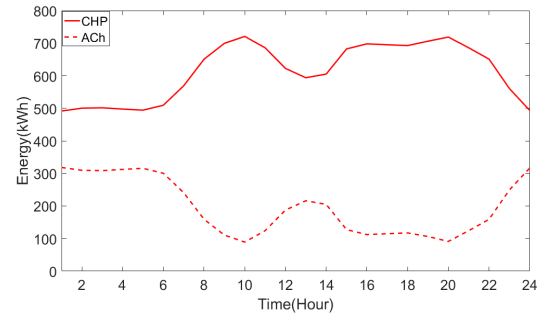


FIGURE 11. Heating conversion in C-EH.

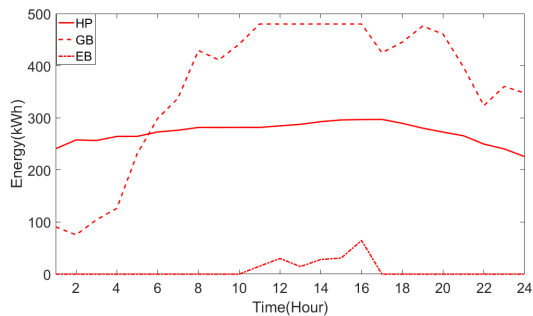


FIGURE 8. Heating conversion in I-EH.

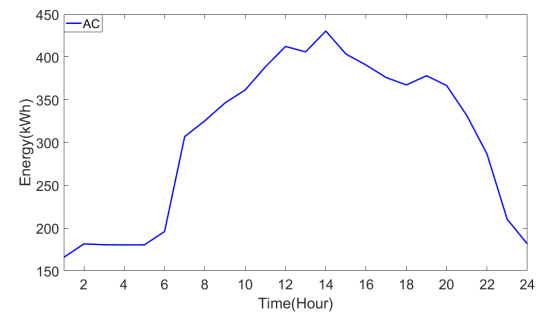


FIGURE 12. Cooling conversion in R-EH.

cooling energy through HP. According to the proposed strategy, fulfillment of cooling load has the priority over heating and electrical load, as shown in Fig. 6. If the electrical load of I-EH exceeds the capacity of RES, the shortage of electricity is supplied from the UG or other EHs, as shown in Fig. 7.

When all electricity generated is consumed by electricity and cooling loads, the heating load must be met by GB. Due to the heat production of AC cannot meet the loads in R-EH, the R-EH must buy heat to help shave heat load. As a contrast, the thermal energy production of HP and GB is sometimes

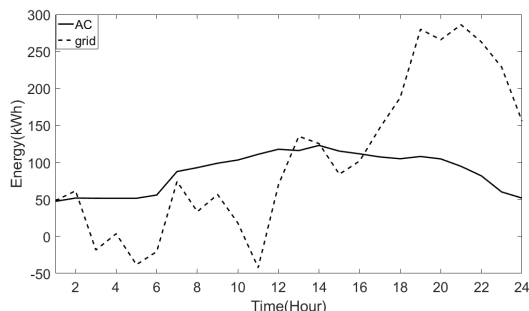


FIGURE 13. Electricity conversion in R-EH.

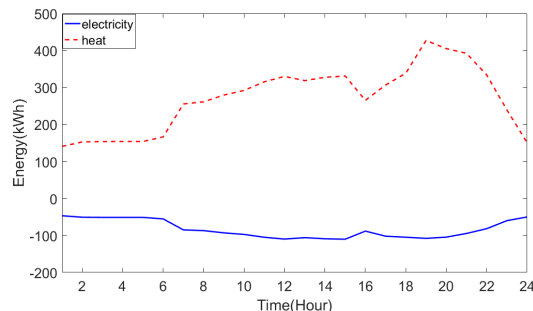


FIGURE 15. Energy exchange among EHs.

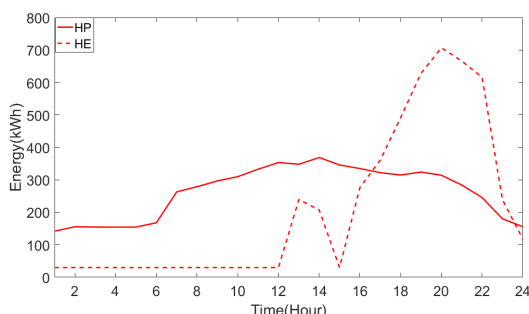


FIGURE 14. Heating conversion in R-EH.

surplus in I-EH, so the I-EH can sell heat to R-EH and EB almost does not work due to the price bidding, as shown in Fig. 8.

Natural gas is mostly used in CHP. The electricity generation of CHP unit is determined based on fulfillment of electrical load, as shown in Fig. 10. The recovered heat from CHP unit can be used for supplying heating load, as shown in Fig. 11. The only extracted heat from CHP can be used by ACh. If thermal energy produced by CHP is not sufficient for meeting cooling load, the RES are assigned the task of supplying the shortage of cooling energy through CC, as shown in Fig. 9. Then, the remainder of available electrical energy is assigned to meet electrical load of the C-EH or sell to other EHs, as shown in Fig. 10.

The Fig. 12-14 demonstrate that it is not cost effective for R-EH to install GB and ACh when the energy required is supplied by I-EH and C-EH. Moreover, it is more efficient to sell electricity to other EHs and utilize AC due to the fact that the RES can provide sufficient electricity. When an ACh is used, a GB must also be installed to generate the heat required by the ACh, thus increasing the cost of R-EH.

C. ENERGY EXCHANGE AMONG EHS

It is demonstrating that the surplus heating energy is supplied by GB and HP of I-EH. As a result, the shortage of electrical energy is supplied by RES of C-EH and R-EH, which can effectively reduce the burden of trading power with UG, as shown in Fig. 15. The statistics of total operating cost in a continuous 24 hours period are shown in table 5.

TABLE 5. Statistics of total operating cost of multi-IES.

Subjects	without Coordination (\$)	with Coordination(\$)	Cost Reduction (%)
I-EH	592.21	608.75	-2.79
C-EH	455.27	414.39	8.98
R-EH	183.81	168.74	8.2
Multi-IES	1231.29	1191.88	3.2

Table 5 shows the cost for each EH and the total multi-IES according to the constraints and the cost results before and after the coordination are compared. This table shows that the results before and after the coordination is applied are different for each EH. The cost of multi-IES without energy coordination is 1231.29\$ per day, and the optimal cost of multi-IES participating in energy coordination is 1191.88\$ per day. In the case of C-EH and R-EH, the cost was reduced due to coordination and the cost for I-EH increased. However, the cost of the entire multi-IES is reduced by nearly 3.2% when the coordination is applied. In other words, the cost of some EHs will increase, but other EHs will benefit, which will contribute to operation efficiency of the entire multi-IES.

TABLE 6. Results obtained from different methods.

Methods	Proposed (\$)	MILP(\$)	MOWOA(\$)
I-EH	608.75	633.75	622.54
C-EH	414.39	477.83	454.13
R-EH	168.74	187.27	178.19
Multi-IES	1191.88	1298.85	1254.86

Solutions provide a comparison among MILP [4], multi-objective whale optimization algorithm (MOWOA) [36] and the propose algorithm in table 6 for accurate objective function minimization. It shows that the proposed algorithm get less cost than MILP and MOWOA. The proposed algorithm has better results in optimizing the operation cost of multi-IES.

V. CONCLUSION

Increasing load, RES generation and emission create a new challenge for the future energy management of Multi-IES. To reduce the disposal of RES and total operating costs of multi-IES, a coordinated operation model based on three-interconnected EHs has been implemented in this paper,

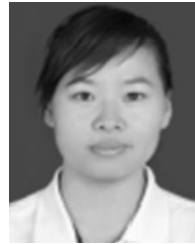
which all IESs are optimized as a community of interests. The uncertainties in demand and RES forecasts were also considered. It is concluded that RES can be incorporated successfully in design of multi-IES, when the complementary performances of RES coupled with energy conversions can provide for the needed flexibility in meeting cooling, heating and electricity loads to achieve the minimum cost for the operation of the multi-IES under the proposed strategy. The study result shows that the coordinated operation of multi-IES has better economic benefits than the isolated operation of each IES. In addition, the proposed strategy leads to lower multi-carrier energy consumption cost, lower peak power and heat demand for multi-IES, which can be further used in the economic and energy efficient operation of energy internet.

REFERENCES

- [1] Y. Wang *et al.*, "Mixed-integer linear programming-based optimal configuration planning for energy hub: Starting from scratch," *Appl. Energy*, vol. 210, pp. 1141–1150, Jan. 2018.
- [2] S. D. Beigvand, H. Abdi, and M. La Scala, "A general model for energy hub economic dispatch," *Appl. Energy*, vol. 190, pp. 1090–1111, Mar. 2017.
- [3] A. Shabanpour-Haghighi and A. R. Seifi, "An integrated steady-state operation assessment of electrical, natural gas, and district heating networks," *IEEE Trans. Power Syst.*, vol. 31, no. 5, pp. 3636–3647, Sep. 2016.
- [4] C. Shao, X. Wang, M. Shahidehpour, X. Wang, and B. Wang, "An MILP-based optimal power flow in multicarrier energy systems," *IEEE Trans. Sustain. Energy*, vol. 8, no. 1, pp. 239–248, Jan. 2017.
- [5] L. Bai, F. Li, H. Cui, T. Jiang, H. Sun, and J. Zhu, "Interval optimization based operating strategy for gas-electricity integrated energy systems considering demand response and wind uncertainty," *Appl. Energy*, vol. 167, pp. 270–279, Apr. 2016.
- [6] N. Holjevac, T. Capuder, N. Zhang, I. Kuzle, and C. Kang, "Corrective receding horizon scheduling of flexible distributed multi-energy microgrids," *Appl. Energy*, vol. 207, pp. 176–194, Dec. 2017.
- [7] S. Skarvelis-Kazakos, P. Papadopoulos, I. G. Unda, T. Gorman, A. Belaidi, and S. Zigan, "Multiple energy carrier optimisation with intelligent agents," *Appl. Energy*, vol. 167, pp. 323–335, Apr. 2016.
- [8] Z. Li, W. Wu, M. Shahidehpour, J. Wang, and B. Zhang, "Combined heat and power dispatch considering pipeline energy storage of district heating network," *IEEE Trans. Sustain. Energy*, vol. 7, no. 1, pp. 12–22, Jan. 2016.
- [9] E. A. M. Ceseña, T. Capuder, and P. Mancarella, "Flexible distributed multienergy generation system expansion planning under uncertainty," *IEEE Trans. Smart Grid*, vol. 7, no. 1, pp. 348–357, Jan. 2016.
- [10] J. H. Zheng, Q. H. Wu, and X. Jing, "Coordinated scheduling strategy to optimize conflicting benefits for daily operation of integrated electricity and gas networks," *Appl. Energy*, vol. 192, pp. 370–381, Apr. 2017.
- [11] A. Zlotnik, L. Roald, S. Backhaus, M. Chertkov, and G. Andersson, "Coordinated scheduling for interdependent electric power and natural gas infrastructures," *IEEE Trans. Power Syst.*, vol. 32, no. 1, pp. 600–610, Jan. 2017.
- [12] P. Dueñas, T. Leung, M. Gil, and J. Reneses, "Closure to discussion on 'Gas-electricity coordination in competitive markets under renewable energy uncertainty,'" *IEEE Trans. Power Syst.*, vol. 30, no. 4, pp. 123–131, Jul. 2015.
- [13] Y. Hu, Z. Bie, T. Ding, and Y. Lin, "An NSGA-II based multi-objective optimization for combined gas and electricity network expansion planning," *Appl. Energy*, vol. 167, pp. 280–293, Apr. 2016.
- [14] X. Zhang, G. G. Karady, and S. T. Ariaratnam, "Optimal allocation of CHP-based distributed generation on urban energy distribution networks," *IEEE Trans. Sustain. Energy*, vol. 5, no. 1, pp. 246–253, Jan. 2014.
- [15] X. Xu, X. Jin, H. Jia, X. Yu, and K. Li, "Hierarchical management for integrated community energy systems," *Appl. Energy*, vol. 160, pp. 231–243, Dec. 2015.
- [16] X. Jin, Y. Mu, H. Jia, J. Wu, X. Xu, and X. Yu, "Optimal day-ahead scheduling of integrated urban energy systems," *Appl. Energy*, vol. 180, pp. 1–13, Oct. 2016.
- [17] C. Lin, W. Wu, B. Zhang, and Y. Sun, "Decentralized solution for combined heat and power dispatch through benders decomposition," *IEEE Trans. Sustain. Energy*, vol. 4, no. 8, pp. 1361–1372, Oct. 2017.
- [18] M. Chaudry, N. Jenkins, M. Qadrdan, and J. Wu, "Combined gas and electricity network expansion planning," *Appl. Energy*, vol. 113, no. 6, pp. 1171–1187, Jan. 2014.
- [19] G. Li, R. Zhang, T. Jiang, H. Chen, L. Bai, and X. Li, "Security-constrained bi-level economic dispatch model for integrated natural gas and electricity systems considering wind power and power-to-gas process," *Appl. Energy*, vol. 194, pp. 696–704, May 2017.
- [20] M. Qadrdan, M. Cheng, J. Wu, and N. Jenkins, "Benefits of demand-side response in combined gas and electricity networks," *Appl. Energy*, vol. 192, pp. 360–369, Apr. 2017.
- [21] X. Zhang, M. Shahidehpour, A. Alabdulwahab, and A. Abusorrah, "Hourly electricity demand response in the stochastic day-ahead scheduling of coordinated electricity and natural gas networks," *IEEE Trans. Power Syst.*, vol. 31, no. 1, pp. 592–601, Jan. 2016.
- [22] I. G. Sardou, M. E. Khodayar, and M. T. Ameli, "Coordinated operation of natural gas and electricity networks with microgrid aggregators," *IEEE Trans. Smart Grid*, vol. 9, no. 1, pp. 199–210, Jan. 2018.
- [23] A. Alabdulwahab, A. Abusorrah, X. Zhang, and M. Shahidehpour, "Coordination of interdependent natural gas and electricity infrastructures for firming the variability of wind energy in stochastic day-ahead scheduling," *IEEE Trans. Sustain. Energy*, vol. 6, no. 2, pp. 606–615, Apr. 2015.
- [24] Z. Wei, S. Chen, G. Sun, D. Wang, Y. Sun, and H. Zang, "Probabilistic available transfer capability calculation considering static security constraints and uncertainties of electricity-gas integrated energy systems," *Appl. Energy*, vol. 167, pp. 305–316, Apr. 2016.
- [25] C. A. Saldarriaga, R. A. Hincapie, and H. Salazar, "A holistic approach for planning natural gas and electricity distribution networks," *IEEE Trans. Power Syst.*, vol. 28, no. 4, pp. 4052–4063, Nov. 2013.
- [26] X. Liu and P. Mancarella, "Modelling, assessment and Sankey diagrams of integrated electricity-heat-gas networks in multi-vector district energy systems," *Appl. Energy*, vol. 167, pp. 336–352, Apr. 2016.
- [27] Z. Pan, Q. Guo, and H. Sun, "Interactions of district electricity and heating systems considering time-scale characteristics based on quasi-steady multi-energy flow," *Appl. Energy*, vol. 167, pp. 230–243, Apr. 2016.
- [28] Y. Li *et al.*, "Optimal stochastic operation of integrated low-carbon electric power, natural gas, and heat delivery system," *IEEE Trans. Sustain. Energy*, vol. 9, no. 1, pp. 273–283, Jan. 2018.
- [29] J. Qiu *et al.*, "A linear programming approach to expansion co-planning in gas and electricity markets," *IEEE Trans. Power Syst.*, vol. 31, no. 5, pp. 3594–3606, Sep. 2016.
- [30] X. Zhang, M. Shahidehpour, A. Alabdulwahab, and A. Abusorrah, "Optimal expansion planning of energy hub with multiple energy infrastructures," *IEEE Trans. Smart Grid*, vol. 6, no. 5, pp. 2302–2311, Sep. 2015.
- [31] S. Bahrami and A. Sheikhi, "From demand response in smart grid toward integrated demand response in smart energy hub," *IEEE Trans. Smart Grid*, vol. 7, no. 2, pp. 650–685, Mar. 2016.
- [32] S. Pazouki, A. Mohsenzadeh, S. Ardalani, and M.-R. Haghifam, "Optimal place, size, and operation of combined heat and power in multi carrier energy networks considering network reliability, power loss, and voltage profile," *IET Gener., Transmiss. Distrib.*, vol. 10, no. 7, pp. 1615–1621, 2016.
- [33] K. Orehounig, R. Evins, and V. Dorer, "Integration of decentralized energy systems in neighbourhoods using the energy hub approach," *Appl. Energy*, vol. 154, pp. 277–289, Sep. 2015.
- [34] S. Saremi, S. Mirjalili, and A. Lewis, "Grasshopper optimisation algorithm: Theory and application," *Adv. Eng. Softw.*, vol. 105, pp. 30–47, Mar. 2017.
- [35] Y. Elahi and M. I. A. Aziz, "Mean-variance-CVaR model of multiportfolio optimization via linear weighted sum method," *Math. Problems Eng.*, vol. 2014, Mar. 2014, Art. no. 104064.
- [36] S. Mirjalili and A. Lewis, "The whale optimization algorithm," *Adv. Eng. Softw.*, vol. 95, pp. 51–67, May 2016.



JINGLU LIU received the B.S. degree in electrical engineering automation from Hohai University in 2013 and the M.S. degree in measurement technology and instruments from Northeastern University, China, in 2015, where he is currently pursuing the Ph.D. degree in power electronics and drives with the School of Information Science and Engineering. His current research interests include distributed renewable energy resources optimization and its applications in microgrids, smart grid, and energy internet.



YANHUA QU received the B.S. degree from Shenyang Ligong University, Shenyang, China, in 1999, and the M.S. degree from Northeastern University, Shenyang, in 2006, where she is currently pursuing the Ph.D. degree. Since 2001, she has been with the Shenyang Institute of Engineering. Her research interests include smart grid, fault diagnosis, electronic technology, power electronics, and power transmission.



ANNA WANG received the B.S., M.S., and Ph.D. degrees in measurement technology and instruments from Northeastern University, Shenyang, China, in 1982, 1988, and 2001, respectively. Since 1994, she has been a Full Professor and a Ph.D. Supervisor with the School of Information Science and Engineering, Northeastern University. Her main research interests are analysis and diagnosis of electrical equipment and power system, optimization analysis technology of smart grid, and electric network control of distributed generation system.



WENHUI WANG received the B.S. and M.S. degrees from the North China University of Science and Technology, Tangshan, China, in 2010 and 2013, respectively. He is currently pursuing the Ph.D. degree in pattern recognition and intelligent system with the School of Information Science and Engineering, Northeastern University, China. His research interests are in computational intelligence and its applications in smart grid, computer vision, and machine learning.

...